



Antibacterial Activity Using Eco-friendly Bio-synthesized Zinc Nanoparticles

Aya Aboelnga^{1*} , Hosam Salaheldin²  and Ashraf Elsayed¹ 



CrossMark

¹Botany department, Faculty of Science, Mansoura University, Mansoura 35516, Egypt

²Biophysics division, Physics department, Faculty of Science, Mansoura University, Mansoura 35516, Egypt

Abstract

The production of zinc oxide nanoparticles (ZnO NPs) by fungi is developing as a critical nanotechnology topic because of its green, eco-friendly, non-toxic, and cost-effective nature. *Fusarium oxysporum*. has been used as a stabilizing and reducing agent in the biosynthesis of ZnO NPs. Various characterization approaches, including UV-Vis spectroscopy and X-ray diffraction (XRD), confirmed the synthesis of ZnO NPs with an average size of 26.3 nm. Furthermore, the micrographs of transmission electron microscopy (TEM) revealed that ZnO NPs had a crystalline structure with hexagonal wurtzite from 5 to 47 nm size. Fourier transform infrared (FTIR) pattern, revealed the presence of reducing and stabilizing agents such as carboxylic acid, and amines. The antibacterial activity of ZnO NPs against Gram-positive and Gram-negative clinical bacterial isolates was remarkable where ZnO NPs have shown strong antibacterial activity against *Salmonella typhi* more than *Escherichia coli*, whereas, at a dosage of 50 mg/ mL, ZnO NPs had slightly more activity against *Bacillus subtilis* than *Staphylococcus aureus*.

Keywords: ZnO NPs, *Fusarium oxysporum*, Antibacterial activity, Biosynthesis.

1. Introduction

According to previous studies, most infectious bacteria are resistant to at least one common antibiotic, but the other ones are also resistant to multiple antibiotics [1]. Antibiotic efficiency is reduced as a result of the emergence of harmful microorganisms that develop antibiotic resistance.

Different effective therapies must be developed to stop the spread of resistant germs to avoid returning to the pre-antibiotic era [2-4]. Not only Gram-positive *S. aureus* is one of the most significant causes of sickness in humans, particularly nosocomial infections but also Gram-negative bacteria *E. coli* and *S. typhi*, which are widely distributed [5-7]. Antibiotic resistance in bacteria caused hospital long-time stays and high concentrations of treatments which might increase the fatality rate [8, 9].

The development of novel, inexpensive, and environmentally friendly bactericidal and/or bacteriostatic agents is required to open up new possibilities for nanoparticles due to their antibacterial activities. On top of that nanoparticles can overcome the pathogenic bacteria's resistance to the antibiotic agents [10, 11]. Nanoparticles (NPs) are very small particles with sizes ranging from 1 to 100 nm that are found in nanoscale materials, considering their minuscule size and high surface-to-volume ratio, they exhibit considerable variances in characteristics from their bulk counterparts. Regarding this, NPs have been cohesive by offering innovative solutions, in numerous sectors. The creation of new synthetic procedures for the synthesis of nanoparticles with varied sizes, shapes, and chemical compositions is one of the prerequisites for the advancement of nanotechnology [12].

*Corresponding author e-mail: ayaaboelnga98@gmail.com (Aya Aboelnga)

Received date 01 June 2023; revised date 07 July 2023; accepted date 31 July 2023

DOI: 10.21608/EJCHEM.2023.214811.8065

©2024 National Information and Documentation Center (NIDOC)

Sol-gel procedure, solvent evaporation technique, interferometric lithography, physical fragmentation, and precipitation from the microemulsion method are a few examples of physical and chemical processes that have been utilized to synthesize NPs [13, 14]. Chemical approaches apply dangerous and poisonous compounds that donate environmental pollution furthermore health hazards. Also, the physical method requires significant energy consumption, pressure, and temperature [15].

For instance, triethyl amine, polyvinyl alcohol (PVA), oleic acid, and ethylenediaminetetraacetic acid (EDTA), which are frequently employed as capping and stabilizing agents to control the size of NPs and prevent them from aggregation, are all unfavorable byproducts of chemical processes [16-20]. Some of these dangerous compounds might be present or bonded in the manufactured NPs. These hazards integrated into the synthesis approach may limit the applications of NPs in humans and animals [13].

The biological method has drawn a lot of attention because it uses less dangerous chemicals and is natural and energy-efficient. The active components from plants and microorganisms, such as bacteria, fungi, and yeasts, are used in the biological synthesis of NPs. This approach is promising because of its efficiency, eco-friendly, mass production, and low cost. In the past ten years, there are an increase in interest in the utilization of microbes, which could be employed as models [21].

Fungi are a good candidate for the synthesis of nanoparticles. Fungi produce nanoparticles with good dispersion and sharp dimensions. Fungi have led research towards biological techniques for metallic nanoparticle synthesis, due to their tolerance and capacity for metal bioaccumulation. They can synthesize a vast number of enzymes, including those necessary for the production of nanoparticles [22].

Due to their high binding capacity, strong tolerance to higher metal concentrations, and superior ability in metal bioaccumulation over bacteria, fungi are a promising approach for the production of zinc NPs [23]. Fungi also showed the ability to release a variety of extracellular redox proteins and enzymes. As a result, this made it easier to convert more metal ions into NPs, which makes them suitable materials for large-scale production [24].

ZnO NPs are an excellent choice for biological

applications since they are non-toxic, easy to fabricate, and environmentally safe. Additionally, zinc sulphate and the other three zinc compounds; zinc oxide, zinc nitrate, and zinc chloride have been recognized as safe materials by the US Food and Drug Administration [25, 26].

Reductase enzymes from *F. oxysporum* showed potentiality towards the productivity of nanoparticles in the reaction mixture. Thiolate-containing organics like cysteine, glutathione, and thioglycolate were utilized as surfactants to maintain the particles suspended when ZnS NPs crystallized [27].

It is noteworthy that *S. aureus* and *B. subtilis* were chosen as Gram-positive bacteria whereas *E. coli* and *S. typhi* were picked as Gram-negative bacteria. *E. coli* is widely distributed in the bodies of mammals and frequently causes acute infection. In addition, it is frequently employed in bacterial research and is the best biological indicator for contamination of drinking water. Pathogenic bacteria *S. aureus* typically colonizes the axillae and gastrointestinal tract [28, 29].

The current research is narrating the synthesis of ZnO NPs using *F. oxysporum* in view to applying against human pathogens through good diffusion and minimum inhibitory concentration (MIC) methods. A green biogenic protocol was conducted for the biosynthesis of ZnO NPs from *F. oxysporum*. Since, this technique was eco-friendly, safe, and cost-effective rather than other synthesis techniques.

2. Experimental (Materials and Methods)

2.1. *F. oxysporum* strain

F. oxysporum strain was kindly obtained from Mycology Lab at the Botany Department, Faculty of Science, Mansoura University, Egypt. This strain was cultured on autoclaved Potato Dextrose Agar (PDA) medium: potato extracts 200 mL, sucrose 20 g, agar 20 g, and then incubated at 25°C for five days [30]. The fungal culture was maintained at 4°C to be used in further biosynthesis processes [31, 32].

2.2. Biosynthesis of nano-zinc by *F. oxysporum*

F. oxysporum biomass was obtained by culturing the fungal agar discs (3-5 discs) in broth medium Maltose Glucose Yeast Peptone (MGYP medium): Malt extract 3 g, Glucose 10 g, Yeast extract 3g and Peptone 5g at 28 °C, 180 rpm, for 5 days incubation. After that, the fungal biomass was filtered and

washed three times with distilled water to remove medium residues [33]. For synthesizing nano-zinc, 10 g of fungal biomass was added to 100 mL of a 5×10^3 M aqueous solution of $\text{ZnSO}_4 \cdot 7\text{H}_2\text{O}$ and incubated at 28°C , 200 rpm for 96 h incubation time. Following nanoparticle synthesis, the reaction solution was filtered to remove the fungal cells before the nanoparticles were dried at 70°C for an overnight period. To eliminate the proteins covering the zinc nanoparticles, the nanoparticles were heated in a muffle at 400°C for 1h followed by further 4 hours.

2.3. Characterization of nano-zinc

UV-Vis spectroscopic absorption measurements were performed at room temperature with a UV-Vis spectrophotometer Jenway (7205, United Kingdom) over the 200-800 nm wavelength range. Fourier transforms infrared (FTIR) transmittance was evaluated in the $450\text{-}4000\text{ cm}^{-1}$ range using Burker Vertex 80 (Germany). X-ray Diffraction (XRD) was used to characterize the crystallinity and phase purity of ZnO NPs using a Rigaku Desktop Miniflex II X-ray powder diffractometer with $\text{CuK}\alpha$ radiation. The XRD pattern of ZnO NPs was examined using Crystallographic Search-Match Version 2 and the ICDD Powder Diffraction File database (International Centre for Diffraction Data). Energy dispersive X-ray diffraction (EDS) analysis was determined using a scanning electron microscopy Joel microscope equipped with 40 kV and equipped with an EDS detector.

2.4. The bacteriostatic activity

2.4.1. Well diffusion method

In a nutshell, agar media (Mueller Hinton) and Petri plates were sterilized in an autoclave at 121°C for 30 min. Then, in a laminar airflow environment under sterile circumstances, 20 mL of agar media were distributed to a uniform depth of 4 mm in Petri plates. After the media had been set up, the bacterial strains from the 18 hours culture were scraped across the agar plates. Corkborers were used to make wells, which were then filled with a 50 μL dose of Zn NPs suspension. To assess the zone of inhibition, the sample-loaded petri dishes were incubated at 37°C for 24 hours.

2.4.2. The minimum inhibitory concentration (MIC)

diffusion plates were used to measure the inhibition zones at different concentrations of nanoparticles. Various concentrations of ZnO NPs

solution precisely (5×10^4 , 5×10^3 , 5×10^2 , and 50 ppm) were inoculated with 0.1 mL of standard inoculum (10^7 CFU/mL) of the tested bacterial strains cultured in the sterilized L.B. broth medium. After that, the bacteria-containing tubes were incubated at 37°C for 24 hours. The control sample has no ZnO NPs. The MIC values expressed the sample concentration necessary to inhibit the microbial species [35].

The microbial species under investigation were obtained from the Bacteriology Lab of the Botany Department, Faculty of Science, Mansoura University, Egypt. ZnO NPs were tested for their activity against both Gram-positive and Gram-negative clinical bacterial strains (*B. subtilis*, *S. aureus*, *S. typhi*, and *E. coli*) according to the good diffusion procedure [34].

3. Results and Discussion

3.1. UV-Vis absorption results

Various spectroscopic methods were used to characterize the formation of ZnO NPs. To assess the optical characteristics of the produced ZnO NPs, UV-Vis detection was performed, where the spectrum revealed a unique peak at 374 nm. Since, the transformation of *F. oxysporum* extract from yellowish to pale violet after, the addition of an aqueous solution of $\text{ZnSO}_4 \cdot 7\text{H}_2\text{O}$ (5×10^3 M) to the *F. oxysporum* extract. Then, the mixture was calcinated at 400°C for 4 hours. Therefore, the main absorption peak of the UV-Vis absorption spectrum of the estimated ZnO NPs could be attributed to the Surface Plasmon vibration ($\lambda_{\text{max}} = 374\text{ nm}$) (Fig.1). The generated ZnO NPs are photoexcited from the valence to the conduction band [36, 37]. These color changes revealed the entire *F. oxysporum* extract interaction and $\text{ZnSO}_4 \cdot 7\text{H}_2\text{O}$ salt produces ZnO NPs primarily and then calcinated later at 400°C .

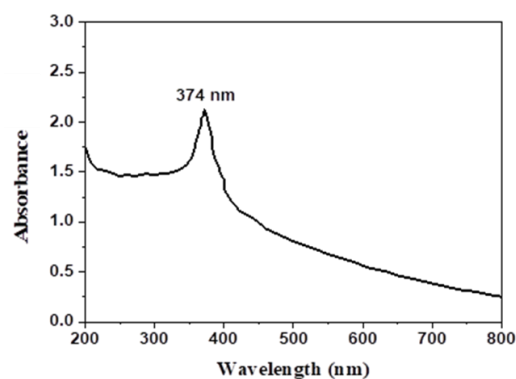


Figure 1: UV–Vis spectrum of ZnO NPs synthesized by *F. oxysporum*.

3.2 FTIR spectroscopy analysis

The pure ZnO NPs' FTIR spectra were observed between 400 and 4000 cm^{-1} . The acquired ZnO NPs' FT-IR spectrum displays the locations and intensities of the peaks, with a broad band between 3600 and 3000 cm^{-1} and a maximum at 3418 cm^{-1} , and a peak at 1637 cm^{-1} attributed to hydrogen-bound O-H stretching vibrations from H₂O or water-molecule bending vibrations of bonded N-H and O-H, respectively [38]. The absorption peaks at 1037, 2850, and 2925 cm^{-1} are attributed to the stretching vibrations of secondary amines. The IR bands in (Fig. 2) are in the range of 1700-600 cm^{-1} and correspond to the vibrations of C=O, C-O, and C-H, respectively [39]. ZnO NPs are considered to have a stretching mode absorption peak between 400 to 600 cm^{-1} . Therefore, the presence of an FT-IR peak at 443 cm^{-1} corresponds to the formation zone of Zn-O [40]. Also, it is known that a fingerprint peak observed around 550 and 650 confirms the presence of the ZnO NPs [41]. Therefore, the band at 618 cm^{-1} is assigned to the ZnO NPs formation.

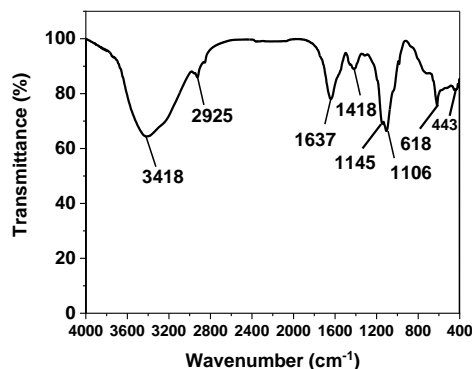


Figure 2: FTIR spectrum of the green synthesized ZnO NPs using *F. oxysporum*.

3.3 X-ray Diffraction (XRD)

The crystalline nature of the nanoparticle was determined using XRD analysis. XRD peaks obtained at 2θ values 31.59°, 34.31°, 36.15°, 47.37°, 56.40°, 62.70° corresponded to lattice planes (100), (002), (101), (102), (110), (103) and depicted the hexagonal wurtzite crystal structure of the nanoparticles (Fig. 3), when compared to the conclusions of the Joint Committee on Powder Diffraction Standards

(JCPDS; card No. 01-089-1397). The diffractogram's data then demonstrated excellent agreement with the hexagonal phase (wurtzite structure). Since, lattice planes (100), (002), and (101) indicate the presence of pure nanoparticles. The nanoparticle sizes were then determined using the Debye-Scherrer equation.

$$D = \frac{K\lambda}{\beta \cos\theta}$$

where D , k , λ , β , and θ represent the average crystal size, shape factor (0.9), the wavelength of the X-ray Cu K α radiation (1.5406 Å), FWHM (full width at half maximum), and Bragg diffraction angle, respectively. The average ZnO NPs crystallite size was calculated as 26.3 nm and also reported by Aalami et al [42]. A small band observed at $2\theta = 25^\circ$ may be attributed to the ZnS NPs that were oxidized to ZnO NPs during the calcination process [43].

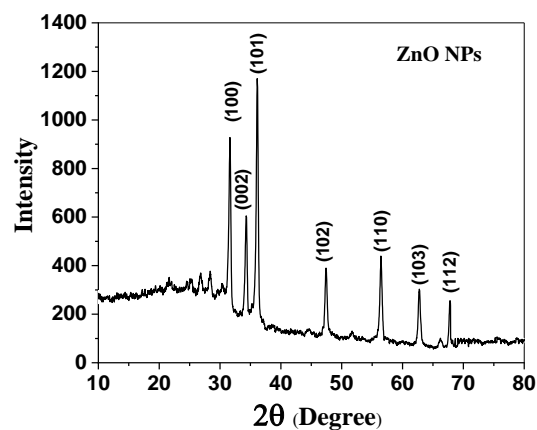


Figure 3: XRD pattern of the synthesized ZnO NPs using *F. oxysporum*.

3.4 Energy dispersive X-ray diffraction (EDX)

The elemental compositions of the biosynthesized ZnO NPs were determined by EDS. Figure 4 shows the presence of ZnO NPs with small traces of sulfide traces that may be attributed to the heating incomplete conversion of ZnS NPs to ZnO NPs at 400 °C as mentioned in the XRD pattern [44].

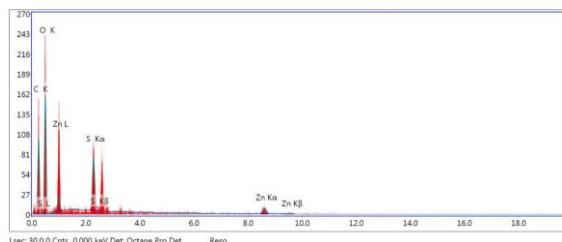


Figure 4: Energy-dispersive X-ray spectroscopy spectrum of ZnO NPs using *F. oxysporum*.

3.5 Transmission Electron Microscopic (TEM)

Figure 5 depicts TEM images of ZnO NPs. The TEM analysis was performed to comprehend the crystalline structure and dimensions of the nanoparticles. ZnO NPs TEM pictures demonstrate the almost hexagonal nature of the particles. According to these photos, the bulk of ZnO NPs have hexagonal shapes and have an average particle size between 5 and 47 nm. The SAED pattern showed that the synthesized ZnO NPs' diffraction rings displayed Debye Scherrer rings with the designations (010), (002), (011), (012), (110), (103), and (112), respectively [45, 46]. The particle size determined by TEM analysis is comparable to that determined by XRD analysis.

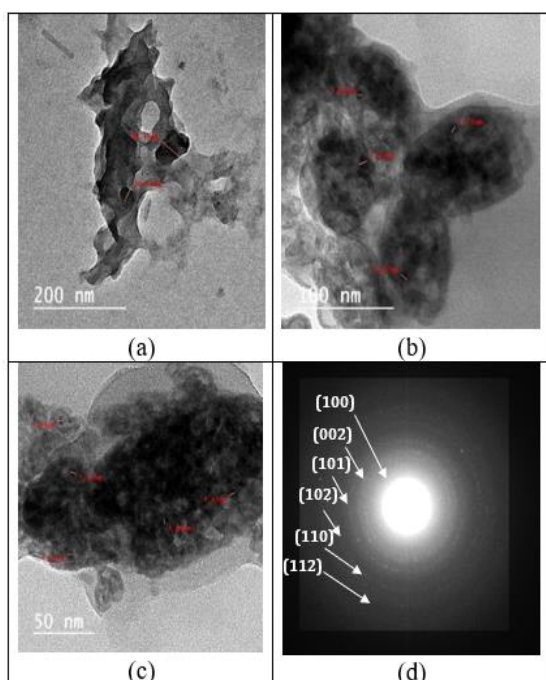


Figure 5: TEM micrographs of ZnO NPs under various magnification scale bars (a) 200 nm (b) 100 nm (c) 50 nm (d) equivalent SAED of single ZnO NP.

3.6 Antibacterial susceptibility test of the tested ZnO NPs

3.6.1 Well diffusion method result

ZnO NPs that were created using *F. oxysporum* were tested for bacteriostatic activity utilizing the good diffusion method. *B. subtilis*, *S. aureus*, *S. typhi*, and *E. coli* were assumed as test organisms for evaluating the impact of the ZnO NPs. ZnO NPs' performance against several bacterial strains and the estimated data are shown in Fig. 6.

The most effective bactericidal results against both *S. typhi* and *B. subtilis* bacteria with ZOI of 22 and 20mm and ZOI of 19 mm were noticed against the *S. aureus*, The least amount of bactericidal action was found against *E. coli*, which had a ZOI of 14 mm with a concentration of 50 μL ZnO NPs.

The bacteriostatic action of ZnO NPs against bacteria could be related to two processes: the penetration of ZnO NPs into the cells which causes the production of reactive oxygen species on their surface as well as the release of Zn^{+2} ions, which break down the cell walls.

The fact that *S. typhi* had the greatest ZOI observed for the ZnO NPs as compared to Gram-positive bacterial strains, gram-negative bacteria have thinner cell walls. This enhances the likelihood that Zn^{+2} ions will reach the *S. typhi* bacteria and destroy them as opposed to Gram-positive bacteria [47].

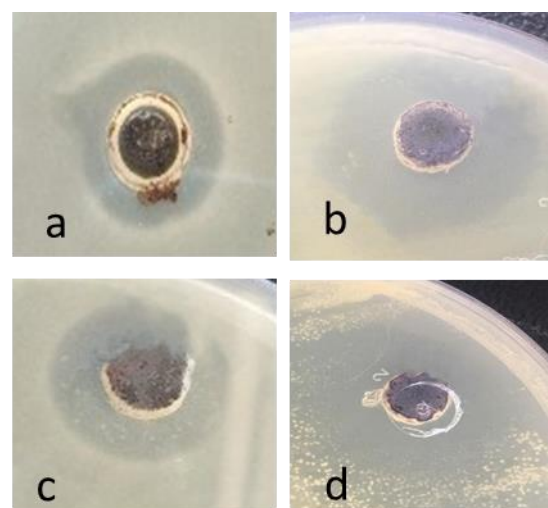


Figure 6: Bacteriostatic activity of ZnO NPs against (a) *E. coli*, (b) *S. typhi*, (c) *S. aureus*, and (d) *B. subtilis* bacteria with ZOI 14,22,19 and 20 mm respectively.

3.6.2 MIC result against ZnO NPs

By measuring microbial growth at a specific concentration of the tested material, the minimum inhibitory concentration (MIC) test was used to assess the antibacterial potency of the biosynthesized Zn NPs made from the *F. oxysporum* extract. The results of the MIC test for nano zinc against *S. aureus* (ATCC 6538), *E. coli* (ATCC 10536), *B. subtilis*, and *S. typhi* bacteria are shown in Table 1. The examined nano zinc solution was generated in a series of dilutions with concentrations of 5×10^4 , 5×10^3 , 5×10^2 , and 50 ppm.

According to the MIC values, the least concentration is required to support the bacteria's development. Instead, it denotes the bare minimal concentration required to inhibit microorganism growth. The control sample shows that the microbial strains are growing naturally. Using this method, it was found that the largest percentage of microbial growth was suppressed by the lowest percentage of turbidity. 200 L of microbial species were added to 2 mL of culture medium to create the culture medium. According to Table 1, MIC data, the sample had a MIC of 5×10^4 ppm when tested against *B. subtilis* and *S. typhi*, but only 5×10^3 ppm when tested against *S. aureus* and *E. coli*. The findings support a recent study conducted on pathogenic, halophilic, and resistant bacterial species [48, 49].

Table 1: MIC of ZnO NPs against the tested bacteria.

Bacterial type	MIC value
<i>E. coli</i>	5×10^3 ppm
<i>B. subtilis</i>	5×10^4 ppm
<i>S. aureus</i>	5×10^4 ppm
<i>S. typhi</i>	5×10^4 ppm

4. Conclusions

F. oxysporum served as the reducing and stabilizing agents in a two-step process for the synthesis of ZnO NPs. XRD was used to characterize the nanoparticles, and the average size was determined to be 26.3 nm. Using TEM image analysis, the almost hexagonal wurtzite nanoparticles were seen. Nanoparticles ranged in size from 5 to 47 nm, according to TEM examination. Results from TEM and XRD were comparable. Additionally, the synthesis of pure ZnO nanocrystals was verified by XRD and EDX analysis. Gram-positive and Gram-negative bacteria are both effectively combatted by ZnO NPs outstanding antibacterial properties. Consequently, this approach would be a low-cost, straightforward, and environmentally friendly way to create ZnO NPs, which might be applied in several pharmaceutical industries.

5. Conflicts of interest

“No conflicts”.

6. Formatting of funding sources

No funding sources

7. References

- [1] Ventola CL. The antibiotic resistance crisis: part 1: causes and threats. *Pharmacy and therapeutics*. 2015 Apr;40(4):277.
- [2] Elmogy S, Ismail MA, Hassan RY, Noureldeen A, Darwish H, Fayad E, Elsaid F, Elsayed A. Biological Insights of Fluoroaryl-2, 2'-Bichalcophene Compounds on Multi-Drug Resistant *Staphylococcus aureus*. *Molecules*. 2020 Dec 30;26(1):139.
- [3] Alfadaly RA, Elsayed A, Hassan RY, Noureldeen A, Darwish H, Gebreil AS. Microbial sensing and removal of heavy metals: Bioelectrochemical detection and removal of chromium (vi) and cadmium (ii). *Molecules*. 2021 Apr 27;26(9):2549.
- [4] Elsayed A, Mohamedin A, Ata T, Ghazala N. Molecular characterization of multidrug resistant clinical *Escherichia coli* isolates. *Am. J. Biochem. Mol. Biol.* 2016;6:72-83.
- [5] Azam A, Ahmed AS, Oves M, Khan MS, Habib SS, Memic A. Antimicrobial activity of metal oxide nanoparticles against Gram-positive and Gram-negative bacteria: a comparative study. *International journal of nanomedicine*. 2012 Dec 5:6003-9.
- [6] Sultan MS, Elsayed A, El-Amir YA. In vitro effect of plant parts extract of *Senecio glaucus* L. On pathogenic bacteria. *Biointerface Res. Appl. Chem.* 2022;12:3800-10.
- [7] Pugazhenthiran N, Murugesan S, Muneeswaran T, Suresh S, Kandasamy M, Valdés H, Selvaraj M, Savariraj AD, Mangalaraja RV. Biocidal activity of citrus limetta peel extract mediated green synthesized silver quantum dots against MCF-7 cancer cells and pathogenic bacteria. *Journal of Environmental Chemical Engineering*. 2021 Apr 1;9(2):105089.
- [8] Finley RL, Collignon P, Larsson DJ, McEwen SA, Li XZ, Gaze WH, Reid-Smith R, Timinouni M, Graham DW, Topp E. The scourge of antibiotic resistance: the important role of the environment. *Clinical infectious diseases*. 2013 Sep 1;57(5):704-10.
- [9] Berendonk TU, Manaia CM, Merlin C, Fatta-Kassinos D, Cytryn E, Walsh F, Bürgmann H, Sørum H, Norström M, Pons MN, Kreuzinger N. Tackling antibiotic resistance: the environmental framework. *Nature reviews microbiology*. 2015 May;13(5):310-7.
- [10] Vickers NJ. Animal communication: when i'm calling you, will you answer too?. *Current biology*. 2017 Jul 24;27(14):R713-5.
- [11] Krishnamoorthy K, Veerapandian M, Zhang LH, Yun K, Kim SJ. Antibacterial efficiency of graphene nanosheets against pathogenic bacteria via lipid peroxidation. *The journal of physical chemistry C*. 2012 Aug 16;116(32):17280-7.
- [12] Heikal YM, Şuţan NA, Rizwan M, Elsayed A. Green synthesized silver nanoparticles induced cytogenotoxic and genotoxic changes in *Allium cepa* L. varies with nanoparticles doses and duration of exposure. *Chemosphere*. 2020 Mar 1;243:125430.
- [13] Agarwal H, Menon S, Kumar SV, Rajeshkumar S. Mechanistic study on antibacterial action of

- zinc oxide nanoparticles synthesized using green route. *Chemico-biological interactions*. 2018 Apr 25;286:60-70.
- [14] Kołodziejczak-Radzimska A, Jesionowski T. Zinc oxide from synthesis to application: a review. *Materials*. 2014 Apr 9;7(4):2833-81.
- [15] Naveed Ul Haq A, Nadhman A, Ullah I, Mustafa G, Yasinzi M, Khan I. Synthesis approaches of zinc oxide nanoparticles: the dilemma of ecotoxicity. *Journal of Nanomaterials*. 2017 Apr 18;2017.
- [16] Kesik M, Kanik FE, Turan J, Kolb M, Timur S, Bahadır M, Toppare L. An acetylcholinesterase biosensor based on a conducting polymer using multiwalled carbon nanotubes for amperometric detection of organophosphorous pesticides. *Sensors and Actuators B: Chemical*. 2014 Dec 15;205:39-49.
- [17] Mundell VJ. Synthesis and functionalisation of metal and metal oxide nanoparticles for theranostics. Nottingham Trent University (United Kingdom); 2013.
- [18] Aboulaich A, Balan L, Ghanbaja J, Medjahdi G, Merlin C, Schneider R. Aqueous route to biocompatible ZnSe: Mn/ZnO core/shell quantum dots using 1-thioglycerol as stabilizer. *Chemistry of Materials*. 2011 Aug 23;23(16):3706-13.
- [19] Nagvenkar AP, Deokar A, Perelshtein I, Gedanken A. A one-step sonochemical synthesis of stable ZnO-PVA nanocolloid as a potential biocidal agent. *Journal of Materials Chemistry B*. 2016;4(12):2124-32.
- [20] Chandrasekaran P, Viruthagiri G, Srinivasan N. The effect of various capping agents on the surface modifications of sol-gel synthesised ZnO nanoparticles. *Journal of Alloys and Compounds*. 2012 Nov 5;540:89-93.
- [21] Gopinath K, Karthika V, Gowri S, Senthilkumar V, Kumaresan S, Arumugam A. Antibacterial activity of ruthenium nanoparticles synthesized using *Gloriosa superba* L. leaf extract. *Journal of Nanostructure in Chemistry*. 2014 Mar;4:1-6.
- [22] Sastry M, Ahmad A, Khan MI, Kumar R. Biosynthesis of metal nanoparticles using fungi and actinomycete. *Current science*. 2003 Jul 25;162:70.
- [23] Ahmad A, Mukherjee P, Senapati S, Mandal D, Khan MI, Kumar R, Sastry M. Extracellular biosynthesis of silver nanoparticles using the fungus *Fusarium oxysporum*. *Colloids and surfaces B: Biointerfaces*. 2003 May 1;28(4):313-8.
- [24] Neethu S, Midhun SJ, Radhakrishnan EK, Jyothis M. Surface functionalization of central venous catheter with mycofabricated silver nanoparticles and its antibiofilm activity on multidrug resistant *Acinetobacter baumannii*. *Microbial pathogenesis*. 2020 Jan 1;138:103832.
- [25] Rosi NL, Mirkin CA. Nanostructures in biodiagnostics. *Chemical reviews*. 2005 Apr 13;105(4):1547-62.
- [26] Vaseem M, Umar A, Hahn YB. ZnO nanoparticles: growth, properties, and applications. *Metal oxide nanostructures and their applications*. 2010;5(1):10-20.
- [27] Lau BL, Hsu-Kim H. Precipitation and growth of zinc sulfide nanoparticles in the presence of thiol-containing natural organic ligands. *Environmental Science & Technology*. 2008 Oct 1;42(19):7236-41.
- [28] Mostafa AA, Al-Askar AA, Almaary KS, Dawoud TM, Sholkamy EN, Bakri MM. Antimicrobial activity of some plant extracts against bacterial strains causing food poisoning diseases. *Saudi journal of biological sciences*. 2018 Feb 1;25(2):361-6.
- [29] Kim JH, Yoo JG, Ham JS, Oh MH. Direct detection of *Escherichia coli*, *Staphylococcus aureus*, and *Salmonella* spp. in animal-derived foods using a magnetic bead-based immunoassay. *Korean Journal for Food Science of Animal Resources*. 2018 Aug;38(4):727.
- [30] Saleh H, Abdelrazak A, Elsayed A, El-Shishtawy H, Osman Y. Optimizing production of a biopesticide protectant by black yeast. *Egyptian Journal of Biological Pest Control*. 2018 Dec;28(1):1-2.
- [31] Elamawi RM, Al-Harbi RE, Hendi AA. Biosynthesis and characterization of silver nanoparticles using *Trichoderma longibrachiatum* and their effect on phytopathogenic fungi. *Egyptian journal of biological pest control*. 2018 Dec;28(1):1-1.
- [32] Linh TM, Mai NC, Hoe PT, Ngoc NT, Thao PT, Ban NK, Van NT. Development of a cell suspension culture system for promoting alkaloid and vinca alkaloid biosynthesis using endophytic fungi isolated from local *Catharanthus roseus*. *Plants*. 2021 Mar 31;10(4):672.
- [33] Apte PS, Deshpande MV, Shankar V. Optimization of medium for extracellular nuclease formation from *Rhizopus stolonifer*. *World Journal of Microbiology and Biotechnology*. 1993 Mar;9:205-9.
- [34] Suresh S, Ilakiya R, Kalaiyan G, Thambidurai S, Kannan P, Prabu KM, Suresh N, Jothilakshmi R, Kumar SK, Kandasamy M. Green synthesis of copper oxide nanostructures using *Cynodon dactylon* and *Cyperus rotundus* grass extracts for antibacterial applications. *Ceramics International*. 2020 Jun 1;46(8):12525-37.
- [35] Hassan A, Rahman S, Deeba F, Mahmud S. Antimicrobial activity of some plant extracts having hepatoprotective effects. *Journal of Medicinal Plants Research*. 2009 Jan 31;3(1):020-3.
- [36] Salaheldin HI, Negm A, Osman GE. Porcine skin gelatin-silver nanocomposites: synthesis, characterisation, cell cytotoxicity, and antibacterial properties. *IET nanobiotechnology*. 2017 Dec;11(8):957-64.
- [37] Al-Mohaimed AM, Al-Onazi WA, El-Tohamy MF. Multifunctional eco-friendly synthesis of ZnO nanoparticles in biomedical applications. *Molecules*. 2022 Jan 17;27(2):579.
- [38] Kamarajan G, Anburaj DB, Porkalai V, Muthuvel A, Nedunchezian G. Green synthesis of ZnO nanoparticles using *Acalypha indica* leaf extract and their photocatalyst degradation and antibacterial activity. *Journal of the Indian Chemical Society*. 2022 Oct 1;99(10):100695.
- [39] Sowri Babu K, Ramachandra Reddy A, Sujatha C, Venugopal Reddy K, Mallika AN. Synthesis and optical characterization of porous ZnO.

- Journal of Advanced Ceramics. 2013 Sep;2:260-5.
- [40] Fouda A, Hassan SE, Abdel-Rahman MA, Farag MM, Shehal-deen A, Mohamed AA, Alsharif SM, Saied E, Moghanim SA, Azab MS. Catalytic degradation of wastewater from the textile and tannery industries by green synthesized hematite (α -Fe₂O₃) and magnesium oxide (MgO) nanoparticles. *Current Research in Biotechnology*. 2021 Jan 1;3:29-41.
- [41] Christobel GJ. Vibrational spectroscopy of ZnO-ZnS nanoparticles. *International Journal of Science and Research*. 2016 Jun;5(6):2228-30.
- [42] Aalami AH, Mesgari M, Sahebkar A. Synthesis and characterization of green zinc oxide nanoparticles with antiproliferative effects through apoptosis induction and microRNA modulation in breast cancer cells. *Bioinorganic chemistry and applications*. 2020 Nov 20;2020.
- [43] Poliukhova V, Khan S, Qiaohong Z, Zhang J, Kim D, Kim S, Cho SH. ZnS/ZnO nanosheets obtained by thermal treatment of ZnS/ethylenediamine as a Z-scheme photocatalyst for H₂ generation and Cr (VI) reduction. *Applied Surface Science*. 2022 Feb 1;575:151773.
- [44] Liu Y, Hu J, Zhou T, Che R, Li J. Self-assembly of layered wurtzite ZnS nanorods/nanowires as highly efficient photocatalysts. *Journal of Materials Chemistry*. 2011;21(41):16621-7.
- [45] Thakur S, Neogi S, Ray AK. Morphology-controlled synthesis of ZnO nanostructures for caffeine degradation and *Escherichia coli* inactivation in water. *Catalysts*. 2021 Jan 5;11(1):63.
- [46] Lakshmeesha TR, Kalagatur NK, Mudili V, Mohan CD, Rangappa S, Prasad BD, Ashwini BS, Hashem A, Alqarawi AA, Malik JA, Abd_Allah EF. Biofabrication of zinc oxide nanoparticles with *Syzygium aromaticum* flower buds extract and finding its novel application in controlling the growth and mycotoxins of *Fusarium graminearum*. *Frontiers in microbiology*. 2019 Jun 12;10:1244.
- [47] Mehmood S, Rehman MA, Ismail H, Mirza B, Bhatti AS. Significance of postgrowth processing of ZnO nanostructures on antibacterial activity against Gram-positive and Gram-negative bacteria. *International journal of nanomedicine*. 2015 Jul 16:4521-33.
- [48] Elsayed A, El-Shamy GM, Attia AA. Biosynthesis, characterization, and assessment of zirconia nanoparticles by *Fusarium oxysporum* species as potential novel antimicrobial and cytotoxic agents. *Egyptian Journal of Botany*. 2022 May 1;62(2):507-22.
- [49] Yassin AY, Abdelghany AM, Salama RS, Tarabiah AE. Structural, optical and antibacterial activity studies on CMC/PVA blend filled with three different types of green synthesized ZnO nanoparticles. *Journal of Inorganic and Organometallic Polymers and Materials*. 2023 Apr 1:1-3.